A Medium Voltage Testbed for the Performance and Function Tests of a 13.8 kV Power Conditioning System Converter

Haiguo Li[1*], Zihan Gao[1], Zhe Yang[1], Cheng Nie[1], Fred Wang[1,2]
[1]Min H. Kao Department of Electrical Engineering and Computer Science, the University of Tennessee, Knoxville, TN, USA
[2]Oak Ridge National Laboratory, Oak Ridge, TN, USA
*hli96@vols.utk.edu

***Abstract*-Medium voltage SiC devices facilitate the development of medium voltage grid-connected power electronics converters. However, it is difficult to test these converters directly on the real medium voltage grid, especially considering abnormal grid conditions, such as grid voltage and frequency variation, and different converter operation modes, such as grid-connected mode and islanded mode. This paper introduces the design and implementation of a medium voltage testbed, which supports tests of medium voltage converters in both grid-connected and islanded mode tests. In the grid-connected mode, the testbed can provide up to 13.8 kV grid voltage, can support the four-quadrant operation, and can emulate different grid conditions, such as voltage and frequency variation. In the islanded mode, the converter under test works as a voltage source and the testbed emulates a three-phase balanced or unbalanced load. Experiment test results are provided to validate the design and capability of the testbed.**

Keywords-Medium voltage testbed, grid-connected converter, abnormal grid conditions, islanded mode

I. INTRODUCTION

Medium voltage (MV) transformer-less (without low-frequency transformer) grid-connected converters are facilitated by the development of MV SiC devices. Testing the performance and functions of these MV converters is as important as the design and building of converters themselves. Approaches used in the literature, to test MV converters, can be divided into three categories.

The first category is to directly or indirectly interface to the MV ac grid. In [1-3], converters are directly connected to the MV ac grid to test. Since the MV ac grid may not be available in some places, especially laboratories, the indirect interface method with transformers is used. In [4-6], step-up transformers are used to generate the MV ac grid from the low voltage (LV) ac grid and passive loads are used at the other terminals (ac or dc) of the MV converters to consume power.

The second category is to get the MV converter supplied from the dc side with LV or MV dc power supplies, and passive (resistive and capacitive) loads are used at the MV ac side [7-9].

However, limitations of the above two categories of MV testbed are:

- The power factor range is usually limited by the passive loads, and it is difficult to achieve a four-quadrant operation.
- With the MV ac grid, only normal conditions can be tested, while some abnormal grid conditions, such as voltage variation and frequency variation cannot be tested. These abnormal condition tests are significant as the grid requirements and grid supports become a critical feature for the grid-connected converters [10].
- Cannot provide different converter operation modes, i.e., islanded and grid-connected modes.
- Not energy efficient because of the adopted passive loads.

Considering these limitations, a third category, which uses another converter to test the built converter, is considered. In [11], two identical converters are parallel connected, and one is used to test the other one. In [12], an MMC-based MV dc testbed has been designed and tested, and it can also be used to generate an ac grid with supply from the dc side. However, these setups are complicated, and building another MV converter as the testbed is also a challenge.

In this paper, an MV testbed combing the transformer approach (the second category) and the converter approach (the third category) is designed, constructed, and tested. Compared to the first and second testbed categories, the proposed testbed addresses all the limitations discussed above, and it can support the four-quadrant operation, normal and abnormal grid condition tests, both grid-connected and islanded mode operation, etc. Compared to the third testbed category, the proposed testbed is simpler, easier to construct and control.

The rest of the paper is organized as follows. First, the MV grid-connected converter to be tested is introduced and the requirements for the testbed are discussed in Section II. Then, the testbed design considerations are presented in Section III. The grid emulator/load emulator control scheme is discussed in Section IV, and the construction and tests are conducted in Section V considering different operation modes and grid conditions. Finally, this paper concludes with Section VI.

II. TESTBED REQUIREMENTS

A. Configuration of the Converter Under Test

The MV testbed is designed for the testing of an MV three-phase four-wire power conditioning system (PCS) converter, which is shown in Fig. 1. The PCS converter is used to connect an 850 V dc (LV dc) grid to a 13.8 kV ac grid (MV ac). A dc/dc stage boosts the 850 V dc to 6.7 kV dc, and two dc/dc converters in each phase are parallel connected at the LV dc side and series connected at the MV ac side through two cascaded H-bridges (CHB). The switching frequency of each device is 10 kHz, and the equivalent switching frequency at the ac side is 40 kHz.

The PCS converter has two operation modes. When the MV ac grid is available, the PCS converter operates in the grid-connected mode, and it exchanges power between the LV dc grid and the MV ac grid. To support the grid, the PCS converter is designed considering grid requirements, such as voltage support, voltage ride-through, frequency ride-through, faults, etc.

When the MV ac grid is unavailable, the PCS converter may operate in the islanded or standby mode, depending on the command from the grid operator. When operating in the islanded mode, the PCS converter works as a voltage source, regulating the MV ac voltage and frequency to support the external balanced/unbalanced ac loads.

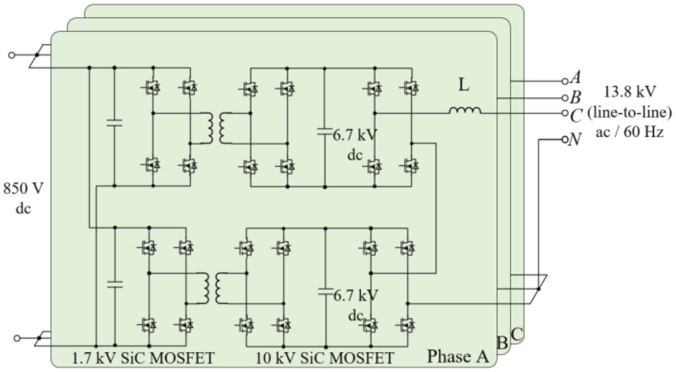

Fig. 1. The PCS converter (equipment under test).

B. Requirements for the Testbed

In general, the testbed should be able to emulate all grid conditions that PCS converter may meet in a real grid, including normal and abnormal grid conditions and different operation modes (grid-connected mode and islanded mode). Also, it needs to be easy to implement and control and to be energy-efficient. The main requirements for the testbed are summarized as follows

- The testbed should form the MV ac grid, regulating the ac voltage and frequency. Also, the testbed should be able to support the four-quadrant operation of the PCS converter.
- To test the grid requirements and grid support functions of the PCS converter, the testbed needs to emulate both the normal and abnormal grid conditions, such as voltage and frequency variations.
- To test the load support function in the islanded mode, the testbed should be able to emulate three-phase balanced and unbalanced loads.
- The testbed should circulate power between the PCS converter and the testbed, so no additional passive loads are needed.
- For safety considerations, the testbed power loop needs to be remotely monitored and controlled.

III. TESTBED DESIGN

A. Testbed Configuration

Based on the requirements, the MV testbed has been designed, as shown in Fig. 2. A 1.7 kV Si IGBT-based two-level three-phase four-wire converter, with a switching frequency of 10 kHz, is used as the LV ac grid emulator. Its dc link is supplied by an LV dc power supply, which is also connected to the LV dc terminals of the PCS converter. The LV ac side of the grid emulator and the MV ac side of the PCS converter are connected by a 277 V to 0-277 V variac and a 120 V to 8 kV / 60 Hz transformer.

Through this connection, the power can circulate between the grid emulator and the PCS converter, so no additional passive loads are needed. Also, bidirectional power circulating flow can be realized, so the four-quadrant operation can be achieved. To emulate the grid-connected mode, the grid emulator controls the ac voltage and frequency, and the PCS converter controls the MV ac-side active and reactive power. To emulate the islanded mode, the PCS converter controls the ac voltage and frequency and the grid emulator controls its active/reactive power.

Since no passive loads are used and the LV dc power supply only needs to compensate the whole losses in the setup, the testbed is energy efficient.

B. LC Filters

Theoretically, no capacitor filter is needed at the converter ac grid side since the main purpose of the test is the control and grid functions verification rather than the power quality. Also, in the real grid application, the L filter is widely used. However, capacitor filters are added at the LV ac grid side and the MV ac grid side considering three factors:

1) Avoid massive core loss and the thermal issue of the 60 Hz transformers

Without the capacitor filters, the high-frequency PWM voltages are directly stressed on the 60 Hz transformers, which induces high-frequency harmonics. Since the 60 Hz transformer cores are silicon steel, which is lossy at high-frequency. Then, the thermal issue could occur and damage the transformers. With the capacitor filter, the high-frequency harmonics can be filtered out, and the voltages on the 60 Hz transformers are sinusoidal.

2) Avoid the winding insulation issue of the 60 Hz transformers

Since the 60 Hz transformers are not designed for high-frequency and high dv/dt PWM voltage, under which the

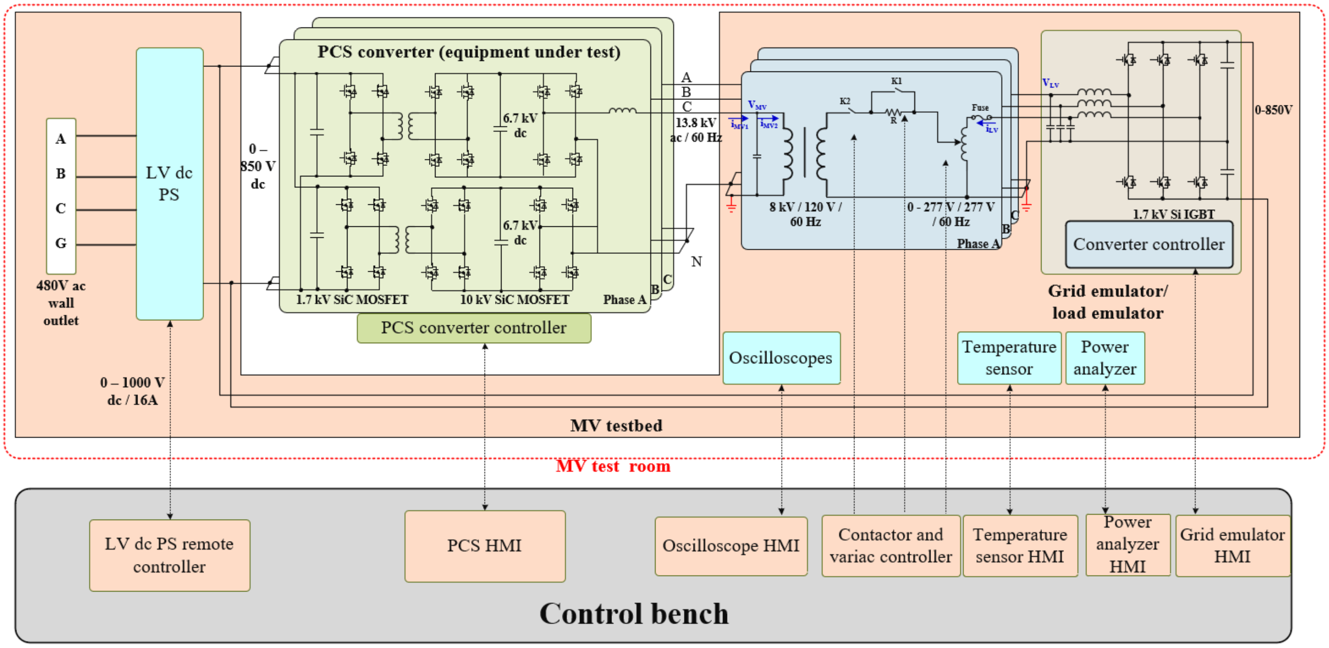

Fig. 2. MV testbed scheme.

transient inter-turn voltage distribution may be greatly uneven, and the turn-to-turn insulation may be damaged. The capacitor filter can reduce the dv/dt of the voltage applied to the transformer windings, and make the voltage distribution among winding turns more even.

3) Avoid resonance between the PCS filter and the parasitic capacitance of the 8 kV/120 V transformer

The parasitic capacitance between one terminal of the MV 60 Hz transformer and the other terminal, which is connected to the chassis and then grounded, is measured to be around 400 pF by an impedance analyzer. Although an integrated capacitance cannot be used to represent the parasitic capacitance, which is distributed among the winding, the resonance frequency between the PCS filter inductor (44 mH) and the parasitic capacitance is estimated to be in the range of tens of kHz. Therefore, resonance can occur after getting excited by the PCS PWM voltage since the equivalent switching frequency of the MV ac side is in that resonance frequency range. The MV ac voltage waveform shown in Fig. 3 confirms the analysis. Even operating at a low voltage, without a capacitor filter, the resonance is obvious. Therefore, a filter capacitor can be used to form an LC filter to filter out the high-frequency harmonics and avoid the resonance.

An 8 nF/14 kV rms ceramic capacitor is used as the filter capacitor at the MV ac side with a series-connected 100 Ω damping resistor (a little underdamped). The crossover frequency of the LC filter formed by the PCS inductor and the filter capacitor is around 8 kHz. The LV ac side filter capacitance is 10 uF, with a series-connected 0.01 Ω damping resistor, and the crossover frequency of the LV side LC filter is 2.3 kHz.

It should be noted that this phenomenon depends on the hardware parameters and may be different in different setups. However, the considerations and solution approaches can be extended to any setup.

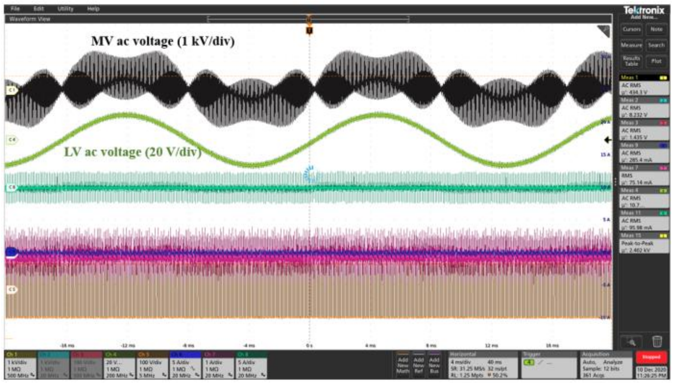

Fig. 3. Resonance waveform between the PCS converter filter inductor and the parasitic capacitor of the 8 kV/ 120 V transformer.

C. Safety Consideration

Safety is always the most significant point, and three main aspects are considered: grounding, remote control, and test procedure.

Grounding is important for insulation and safety concerns. At the LV side, the LV dc middle point is grounded at the grid emulator side. At the MV side, the neutral point of the PCS converter, which is also the neutral point of the three MV transformers is grounded. Also, all the equipment chassis are grounded.

The power loop and the control bench are physically separated. All the power-loop equipment locate in an MV test room, which is labeled with a red dash line in Fig. 2. The control bench, on which the experiment tests are conducted, is outside of the MV room. The LV dc power supply, contactors, variacs, the grid emulator, oscilloscopes, the PCS converter, etc. are all remotely controlled/accessed from the control bench. During the test, no one will be allowed to be in the MV test room.

A test procedure needs to be documented and followed. The proper startup, testing, shut down, system configuration modification, and emergency shutdown procedures are determined. Many safety rules, such as the two-person rule, proper personal protective equipment (PPE), etc. also need to be followed.

D. Protection

Protection is another significant concern in the testbed. Several protection schemes, including hardware and software, are implemented to protect the testbed and the converter under test, as shown in Table 1. Ac overcurrent, ac overvoltage, dc overvoltage protections are realized in the grid emulator based on both software and hardware. These protections are in the microsecond level and can be used as transient overcurrent and overvoltage protection for the testbed and the converter under test. Contactors also have fault current interruption capability, and fuses are installed in the variac. These protection schemes are in the millisecond level and can be used as overload protection. Overcurrent and overvoltage protection are also embedded in the LV dc power supply, which can directly shut down the system from the source side.

Table 1: Testbed protections.

Equipment	**Protection**	**Protection type**	**Response speed**
Three-phase two-level converter	AC overcurrent protection	Hardware	* us
		Software	*** us
	AC overvoltage protection	Hardware	* us
		Software	*** us
	DC overvoltage protection	Hardware	* us
		Software	*** us
Variac fuse	Overcurrent protection	Hardware	** ms
Contactor	Overcurrent protection	Hardware	** ms
LV DC power supply	Overcurrent protection	NA	*** us
	Overvoltage protection	NA	*** us

IV. CONTROL OF THE GRID EMULATOR/LOAD EMULATOR

A. The Grid Emulator Control Scheme

The main function of the testbed in the grid-connected mode test is to emulate the ac grid, controlling the voltage and frequency, including both the normal and the abnormal conditions.

Although closed-loop control gives more accurate output, it slows down the voltage regulation speed and some fast transient conditions cannot be provided. Therefore, open-loop control is adopted in this testbed, and the voltage drop caused by the IGBT and the filter inductor can be treated as the voltage loss on the grid transmission/distribution line.

Two implement approaches are considered to regulate the ac grid voltage, as shown in Fig. 4. The first one is to directly give the three-phase instantaneous grid voltage command, and then the duty cycle of each phase can be calculated as

$$\boldsymbol{D_{abc}} = \frac{2}{V_{dc}}\boldsymbol{V_{abc\_ref}} = \frac{2}{V_{dc}}\boldsymbol{V_{abc\_command}} \tag{1}$$

where $\boldsymbol{D_{abc}}$, $\boldsymbol{V_{abc\_ref}}$, and $\boldsymbol{V_{abc\_command}}$ are the three-phase duty cycle, voltage reference, and voltage command vectors, respectively, i.e.,

$$\boldsymbol{D_{abc}} = \begin{bmatrix} D_a \\ D_b \\ D_c \end{bmatrix};\ \boldsymbol{V_{abc\_ref}} = \begin{bmatrix} V_{a\_ref} \\ V_{b\_ref} \\ V_{c\_ref} \end{bmatrix};\ \boldsymbol{V_{abc}} = \begin{bmatrix} V_{a\_command} \\ V_{b\_command} \\ V_{c\_command} \end{bmatrix} \tag{2}$$

This approach is more suitable to emulate some voltage spikes, dips, swells, etc, which cannot be easily represented through positive-sequence, negative-sequence, and zero-sequence. However, this approach needs to give the voltage command in each switching cycle, which can be realized by either programming the data in the controller or sending the data to the controller through real-time communication.

The second approach is giving the voltage command in positive, negative, and zero sequences, and then calculating the voltage reference for each phase. Besides, the angle information is also needed, which can be obtained according to the frequency command as

$$\boldsymbol{\theta_{pn0}} = \begin{bmatrix} \theta_p \\ \theta_n \\ \theta_0 \end{bmatrix} = \begin{bmatrix} \sum 2\pi f_{command} T_s \\ -\sum 2\pi f_{command} T_s \\ \sum 2\pi f_{command} T_s \end{bmatrix} + \begin{bmatrix} 0 \\ \theta_{n\_init} \\ \theta_{0\_init} \end{bmatrix} \tag{3}$$

where $\boldsymbol{\theta_{pn0}}$ is the angle vector; θ_p, θ_n, and θ_0 are the positive-sequence, negative-sequence, and zero-sequence angles, respectively; $f_{command}$ is the frequency command; θ_{n_init} and θ_{0_init} are the initial angles of the negative-sequence and zero-sequence respectively.

With the angle and the voltage command, the voltage reference of each phase can be calculated as

$$\boldsymbol{V_{abc\_ref}} = \begin{bmatrix} \cos\theta_p & \cos\theta_n & \cos\theta_0 \\ \cos(\theta_p - \frac{2\pi}{3}) & \cos(\theta_n - \frac{4\pi}{3}) & \cos\theta_0 \\ \cos(\theta_p - \frac{4\pi}{3}) & \cos(\theta_n - \frac{2\pi}{3}) & \cos\theta_0 \end{bmatrix} \begin{bmatrix} V_{p\_command} \\ V_{n\_command} \\ V_{0\_command} \end{bmatrix} \tag{4}$$

where $V_{p\_command}$, $V_{n\_command}$, and $V_{0\_command}$ are the positive-sequence, negative-sequence, and zero-sequence voltage commands, respectively. This approach does not require real-time voltage command, and it is more suitable for the grid fault emulation, where the voltage in different sequences can be easily obtained.

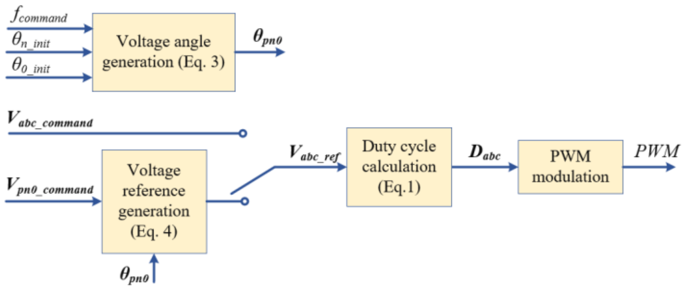

Fig. 4. Grid emulator control scheme.

B. The Load Emulator Control Scheme

Since the load emulator needs to emulate three-phase unbalanced loads, single-phase control is adopted. As shown in Fig.5, the active and reactive power commands are given for each phase, and the grid voltage phase angle is also locked in each phase independently. By doing the control in each phase, there is no need to decouple the positive-sequence, negative-sequence, and zero-sequence voltage and current in the unbalanced case.

Based on the power command and the PLL output, the phase A current reference, I_{aref}, can be calculated as

$$I_{aref} = \frac{P_{aref}}{V_{ad}} \cos\theta_a + \frac{Q_{aref}}{V_{ad}} \sin\theta_a \qquad (5)$$

where P_{aref}, Q_{aref} are the active and reactive power commands in per unit, respectively; V_{ad} is the phase A voltage in per unit; θ_a is the phase A voltage angle. The current reference of phases B and C can be calculated with the same equation.

PR controller is used to regulate the load emulator output current, and the voltage feedforward is adopted to increase the response speed.

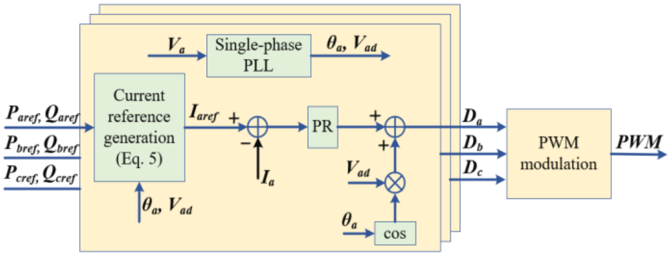

Fig. 5. Load emulator control scheme.

V. TESTBED CONSTRUCTION AND EXPERIMENT TEST

A. Setup Hardware

The testbed is constructed, and the setup picture is shown in Fig. 6. The control bench is outside of this room, and all equipment is remotely controlled/accessed.

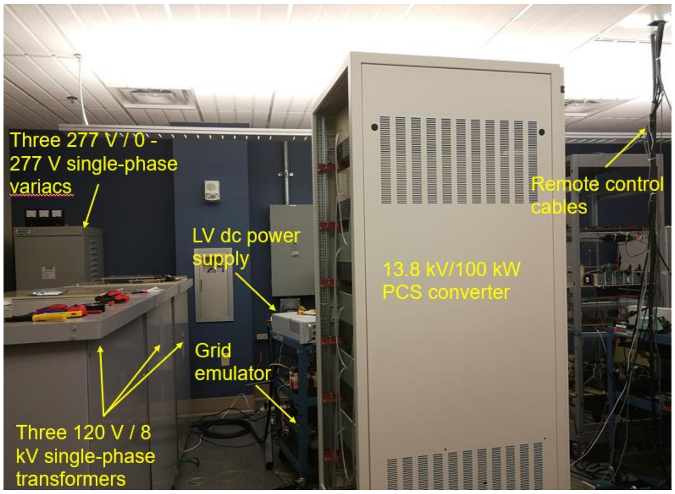

Fig. 6. MV testbed hardware figure.

B. Testbed Test Without the PCS Converter

The MV testbed is first tested without the PCS converter, forming the 13.8 kV ac grid voltage. As shown in Fig. 7, the grid emulator output 240 V RMS phase-to-ground voltages and the MV-side phase-to-ground voltages V_{A_MV}, V_{B_MV}, and V_{C_MV} are all around 8 kV RMS, and the corresponding line-to-line voltage is 13.8 kV. The magnetizing currents are not pure sinusoidal due to the saturation of the MV transformer.

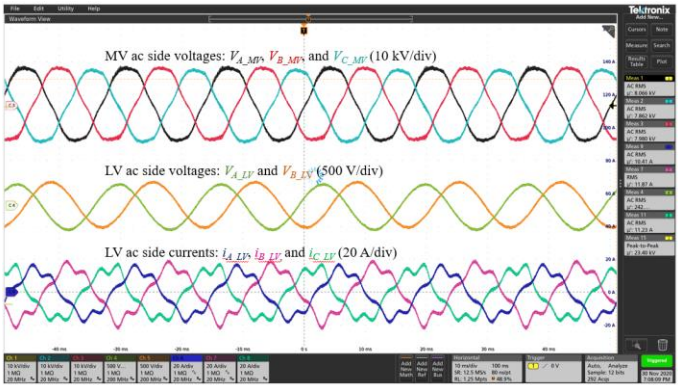

Fig. 7. Medium voltage testbed waveforms without the PCS converter.

C. PCS Converter Islanded Mode Tests

The three-phase PCS converter is then tested in the islanded mode, regulating the MV ac voltage and current to support the external ac loads. The MV side ac voltage and current waveforms, supporting the three-phase balanced load, are shown in Fig. 8. The three-phase voltage and current are all balanced. The waveforms in the unbalanced load support test (phase A and B have loads but phase C has no load) are shown in Fig. 9. Since the PCS converter also needs to provide the magnetizing current of the transformer, phase C still has a little current. Although the three-phase loads are unbalanced, the three-phase voltages, maintained by the PCS converter, are still balanced, which verifies the PCS unbalanced load support capability.

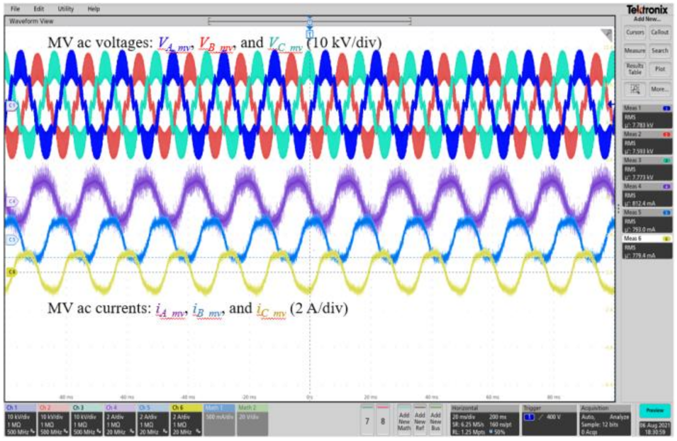

Fig. 8. Balanced ac load support waveforms in the islanded mode.

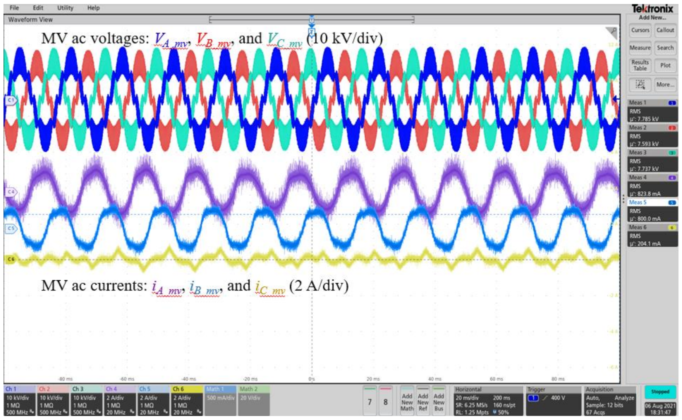

Fig. 9. Unbalanced ac load support waveforms in the islanded mode.

D. PCS Converter Grid-connected Mode Tests

Then, the PCS converter is tested in the grid-connected mode, and some grid functions are tested. The MV-side three-phase ac voltage and current and the LV-side line-to-line voltage during the frequency variation are shown in Fig. 10. In the beginning, the grid voltage is 60 Hz. At time t_1, the grid emulator controls the grid voltage frequency dropping from 60 Hz to 56 Hz within one and a half fundamental cycle (24 ms), and the PCS converter rides through the frequency change. At time t_2, the grid voltage frequency further drops from 56 Hz to 53 Hz with the same frequency change rate, the PCS converter also rides through the frequency change again. At time t_3, the grid voltage frequency drops from 53 Hz to 48 Hz, and the PCS converter under-frequency protection, which is set at 50 Hz, is triggered.

The waveforms during low voltage ride-through are shown in Fig. 11. The grid emulator controls the grid voltage changing from 3.3 kV to 1.65 kV at time t_4 and lasting for 2 s and then recovering to 3.3 kV at time t_5. The PCS converter rides through the low voltage period. The voltage waveforms show some resonance, which is caused by the LC filter due to under damping. It can be improved with more damping resistance.

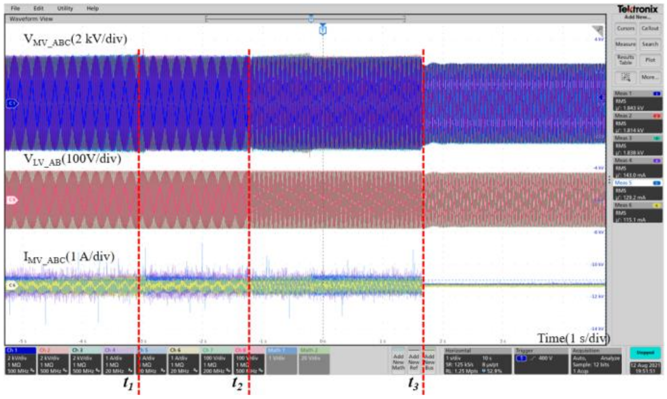

Fig. 10. Frequency ride-through and protection test waveforms.

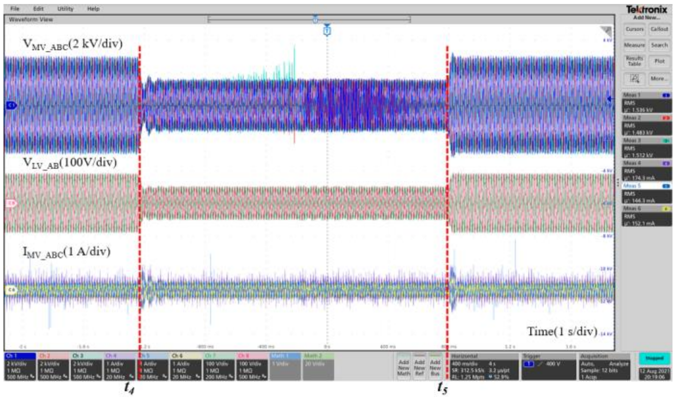

Fig. 11. Low voltage ride-through test waveforms.

VI. CONCLUSION

This paper has discussed the design, construction, and test of an MV testbed for a 13.8 kV PCS converter. The testbed is simple to implement and easy to control. It utilizes an LV three-phase two-level converter as the grid emulator or load emulator in different test modes. For safety consideration, the power loop and the control bench are separated, and all the equipment is remotely controlled/accessed. Also, different types of protection based on hardware and software are implemented. The testbed can support both grid-connected mode and islanded mode tests. In the grid-connected mode, the testbed provides up to 13.8 kV ac grid, supporting the four-quadrant operation and abnormal grid conditions, such as voltage and frequency variations. In the islanded mode, the testbed can emulate three-phase balanced or unbalanced loads. Through circulating power between the testbed and the converter under test, this testbed is energy efficient and does not need extra passive loads. The testbed has been tested under three-phase normal operation individually and together with the MV PCS converter in both the grid-connected mode and the islanded mode, which verifies the design.

ACKNOWLEDGMENT

This work was supported primarily by the Advanced Manufacturing Office (AMO), United States Department of Energy, under Award no. DE-EE0008410. This work made use of the shared facilities of the Engineering Research Center

Program of the National Science Foundation and the Department of Energy under NSF Award no. EEC-1041877. The authors would like to acknowledge the contribution of Southern Company and Powerex.

REFERENCES

[1] T. Liu *et al.*, "Design and Implementation of High Efficiency Control Scheme of Dual Active Bridge Based 10 kV/1 MW Solid State Transformer for PV Application," *IEEE Transactions on Power Electronics,* vol. 34, no. 5, pp. 4223-4238, 2019.

[2] D. Wang *et al.*, "A 10-kV/400-V 500-kVA Electronic Power Transformer," *IEEE Transactions on Industrial Electronics,* vol. 63, no. 11, pp. 6653-6663, 2016.

[3] C. Zhao *et al.*, "Power Electronic Traction Transformer—Medium Voltage Prototype," *IEEE Transactions on Industrial Electronics,* vol. 61, no. 7, pp. 3257-3268, 2014.

[4] S. Madhusoodhanan *et al.*, "Solid-State Transformer and MV Grid Tie Applications Enabled by 15 kV SiC IGBTs and 10 kV SiC MOSFETs Based Multilevel Converters," *IEEE Transactions on Industry Applications,* vol. 51, no. 4, pp. 3343-3360, 2015.

[5] X. She, X. Yu, F. Wang, and A. Q. Huang, "Design and Demonstration of a 3.6-kV–120-V/10-kVA Solid-State Transformer for Smart Grid Application," *IEEE Transactions on Power Electronics,* vol. 29, no. 8, pp. 3982-3996, 2014.

[6] M. Lee, C. Yeh, O. Yu, J. Kim, J. Choe, and J. Lai, "Modeling and Control of Three-Level Boost Rectifier Based Medium-Voltage Solid-State Transformer for DC Fast Charger Application," *IEEE Transactions on Transportation Electrification,* vol. 5, no. 4, pp. 890-902, 2019.

[7] S. Ji, L. Zhang, X. Huang, J. Palmer, F. Wang, and L. M. Tolbert, "A Novel Voltage Balancing Control With dv/dt Reduction for 10-kV SiC MOSFET-Based Medium Voltage Modular Multilevel Converter," *IEEE Transactions on Power Electronics,* vol. 35, no. 11, pp. 12533-12543, 2020.

[8] J. Thoma, B. Volzer, D. Kranzer, D. Derix, and A. Hensel, "Design and Commissioning of a 10 kV Three-Phase Transformerless Inverter with 15 kV Silicon Carbide MOSFETs," in *20th European Conference on Power Electronics and Applications (EPE'18 ECCE Europe)*, 2018, pp. P.1-P.7.

[9] D. Rothmund, T. Guillod, D. Bortis, and J. W. Kolar, "99.1% Efficient 10 kV SiC-Based Medium-Voltage ZVS Bidirectional Single-Phase PFC AC/DC Stage," *IEEE Journal of Emerging and Selected Topics in Power Electronics,* vol. 7, no. 2, pp. 779-797, 2019.

[10] "IEEE Standard for Interconnection and Interoperability of Distributed Energy Resources with Associated Electric Power Systems Interfaces," *IEEE Std 1547-2018 (Revision of IEEE Std 1547-2003),* pp. 1-138, 2018.

[11] D. Dong, M. Agamy, J. Z. Bebic, Q. Chen, and G. Mandrusiak, "A Modular SiC High-Frequency Solid-State Transformer for Medium-Voltage Applications: Design, Implementation, and Testing," *IEEE Journal of Emerging and Selected Topics in Power Electronics,* vol. 7, no. 2, pp. 768-778, 2019.

[12] M. M. Steurer *et al.*, "Multifunctional Megawatt-Scale Medium Voltage DC Test Bed Based on Modular Multilevel Converter Technology," *IEEE Transactions on Transportation Electrification,* vol. 2, no. 4, pp. 597-606, 2016.